Progress In Electromagnetics Research C, Vol. 52, 53–62, 2014

MIMO Antenna for Bluetooth, Wi-Fi, Wi-MAX and UWB Applications

Shilpa Kharche[1, *], Gopi S. Reddy[1], Biswajeet Mukherjee[2], Rajiv Gupta[3], and Jayanta Mukherjee[1]

Abstract—A Multiple Input Multiple Output (MIMO) antenna consisting of two 90° angularly separated semicircular monopoles with steps for Bluetooth, Wi-Fi, Wi-MAX and UWB applications is proposed. Initially, an array of two coplanar circular monopoles with element separation of 25 mm is investigated. In this configuration, mutual coupling is < -5 dB and < -10 dB over 2 GHz–3 GHz and 3 GHz–10.6 GHz, respectively. Mutual coupling is reduced by using 90° angularly separated semicircular monopoles. With semicircular configuration, though the mutual coupling is improved, impedance bandwidth is reduced due to reduction in electrical length. A step like structure is introduced in the semicircular monopoles, and ground plane is modified and extended between the two elements to improve the impedance bandwidth and mutual coupling. Impedance bandwidth from 2.0 GHz–10.6 GHz with $S_{21} < -20$ dB and -14 dB is achieved over 3.1 GHz–10.6 GHz and 2.0–3.1 GHz respectively. The antenna is fabricated using 46 mm × 37 mm RT Duroid substrate. Measurement results agree with the simulation ones. Radiation patterns are stable, and correlation coefficient is < 0.02 over 2.0–10.6 GHz.

1. INTRODUCTION

Recently, Multiple Input Multiple Output (MIMO) systems have emerged as an extension of antenna array to improve channel capacity, spectral efficiency and multipath fading. The performance of MIMO antenna depends on the inter-element spacing, array geometry, radiation pattern of single antenna element, aperture area and number of antenna elements. However, designing MIMO antenna over wide bandwidth is challenging tasks due to the tradeoff between inter-element spacing and mutual coupling. Mutual coupling and radiation patterns are governed by electrical separation between elements, which varies significantly with frequency over wide bandwidth. Larger inter-element spacing results in lower mutual coupling, but the size of the antenna becomes large which is not suitable for compact systems. Decrease in interelement spacing makes an antenna system compact but increases mutual coupling due to increase in surface wave coupling between the elements [1–7].

Several techniques have been proposed to reduce mutual coupling between the closely spaced antennas [1–7]. A reactive transmission line with varying characteristic impedance T lines connected between the lines feeding the antennas is used to reduce the mutual coupling effect in [1]. Mutual coupling due to the excitation of surface waves can be suppressed by using Electromagnetic Band Gap structures (EBG) as shown in [2, 3]. Significant isolation is achieved using EBG, but it suffers from complexity in design and large area of the antenna. As shown in [4, 5], Defected Ground Structures (DGS) are used to reduce mutual coupling between elements where a resonating dumbbell shape is etched in ground plane. DGS based antennas are compact in shape over EBG structures. Single negative magnetic (MNG) metamaterials have been proposed to de-correlate the antennas in [6, 7]. Among them, split ring resonators are used to create MNG layer. High isolation is achieved using an

Received 11 April 2014, Accepted 13 July 2014, Scheduled 17 July 2014

* Corresponding author: Shilpa Kharche (shilpaukharche@gmail.com).

[1] Electrical Engineering Department, Indian Institute of Technology, Bombay, India. [2] Indian Institute of Information Technology, Jabalpur, India. [3] Terna Engineering College, Nerul, Navi Mumbai, India.

ensemble of resonators, comprising the MNG layer for decoupling. However, all these techniques are applicable to narrow bandwidth.

Different techniques have been proposed to reduce the mutual coupling over wide band width [8–14]. A Y-shape stub placed at ground is used in [8] to reduce the mutual coupling between the elements of linear array of two identical ultra wideband (UWB) (3.1 GHz–10.6 GHz) circular monopole antennas. Mutual coupling and correlation coefficient less than −15 dB and −20 dB respectively are achieved with antenna size of $68 \times 40\,\text{mm}^2$ over 3.1 GHz–10.6 GHz. A sleeve coupled stepped impedance resonator placed at ground is used in [9] to improve the isolation. With this, higher isolation of 23 dB is achieved over the bandwidth ranging from 3.1 GHz–10 GHz with antenna size of $62 \times 38\,\text{mm}^2$. A MIMO system using UWB antenna elements with individual ground for each element is proposed in [10]. This achieves a mutual coupling and correlation coefficient of less than −17 dB and −22 dB respectively over 3.1 GHz–10.6 GHz with a comparatively large antenna size of $91 \times 38\,\text{mm}^2$. A UWB MIMO/diversity antenna with tree-like structure to enhance isolation is proposed in [11]. Mutual coupling less than −16 dB is achieved over 3.1 GHz–10.6 GHz with the antenna size of $35 \times 40\,\text{mm}^2$. However, a complicated treelike multi-resonant structure has to be designed to decouple the antenna elements. In [12], a fork-shaped structure is introduced in the ground plane to achieve the isolation of 20 dB with considerably small antenna size of $35 \times 40\,\text{mm}^2$. However, the antenna operates over the bandwidth ranging from 4.4 GHz–10.7 GHz. Inter-element isolations of 26 dB and 20 dB are achieved in [13, 14] respectively, but the antennas are designed over 3.1 GHz–5.15 GHz for a specific applications viz USB dongle and portable devices. The Bluetooth/UWB dual band diversity antenna reported in [15] uses a set of vertical microstrip lines between antenna elements to reduce the mutual coupling.

MIMO antenna with different polarizations is investigated in [16]. Isolation of 15 dB is achieved over the frequency band of 3.1 GHz–10.6 GHz. MIMO UWB antennas with mutual coupling less than −10 dB and −15 dB with inter-element spacing of 43.5 mm and 37.8 mm for parallel feed and orthogonal feed respectively are presented in [17]. However, orthogonally fed antennas suffer from feed complications in a compact communication system.

In this paper, an MIMO antenna comprising two 90° angularly separated semicircular monopole with steps on a modified and extended ground plane for Bluetooth, Wi-Fi, Wi-MAX and UWB applications is proposed. The geometry is derived from an array of UWB circular monopole antennas. The circular monopole antenna array is modified to form two 90° angularly separated semicircular monopole antennas to improve the isolation and achieves the space diversity. Steps are introduced in the geometry to achieve the required impedance bandwidth. The ground plane is further modified and extended to reduce the coupling between the elements, and the structure is optimized to achieve the impedance bandwidth over 2 GHz–10.6 GHz. The fabricated antenna has substrate dimensions of 46 mm × 37 mm with mutual coupling less than −20 dB and less than −14 dB over 3.1 GHz–10.6 GHz and 2 GHz–3.1 GHz bands, respectively.

2. ANTENNA GEOMETRY AND DESIGN THEORY

The various MIMO antenna structures used in evolution process of the proposed UWB MIMO diversity antenna system are shown in Figure 1(a). All the antennas are designed on 0.787 mm thick RT duroid substrate of dielectric constant 2.2 and loss tangent 0.0009. The structures are simulated using method of moment based Zealand IE3D 14.0 software [18].

Antenna 1 in Figure 1(a) consists of two radiators positioned symmetrically with respect to Y axis and fed by 50 Ω microstrip lines of 2.38 mm widths. The radius 'R' of circular monopole in cm is calculated by using (1) [19]

$$f_L = \frac{7.2}{(2.25 \times R) + g}\,\text{GHz} \tag{1}$$

where, "g" is the gap between radiating patch and ground plane in cm, and "f_L" is the lowest resonant frequency corresponding to VSWR = 2. The gap between ground plane and radiating monopole also acts as a matching network.

Antenna 1 is designed with radius $R = 10.2$ mm using (1). Due to the higher current density at the edge of the ground plane, length of ground plane affects impedance bandwidth and radiation pattern more than the width of the ground plane [20]. The length of the ground plane is increased to

accommodate the second element which results in the improvement of impedance bandwidth at lower frequencies. The ground plane dimensions and gap are optimized to achieve impedance bandwidth between 2 GHz–10.6 GHz. Inter-element spacing, as shown in Figure 1(b), is fixed to 25 mm which is $0.5\lambda_0$ where λ_0 is the free space wavelength at 6 GHz. Simulated S_{11}, S_{21} and impedance variation with frequency of Antenna 1, Antenna 2, Antenna 3 and the proposed structure are shown in Figure 2. For Antenna 1, S_{21} less than -10 dB is obtained over UWB. However, S_{21} is greater than -10 dB between 2 GHz–3 GHz. S_{21} increases with decrease in frequency due to decrease in electrical separation between the elements. The geometry is then modified to reduce mutual coupling resulting in Antenna 2 as shown in Figure 1(a). Antenna 2 consists of two 90° angularly separated semicircular monopoles. This increases the electrical separation between two radiators resulting in decrease in mutual coupling. Return loss degrades due to decrease in current path length, but mutual coupling is less than -10 dB over the 2 GHz–3 GHz band and less than -15 dB over UWB. Current is concentrated mainly along the periphery of the semicircular monopole antennas. By increasing the perimeter of the radiating patch, the current path length can be increased to achieve better impedance matching [21]. Therefore, steps are introduced in the angularly separated semicircular monopole elements to increase the current path length resulting in Antenna 3 as shown in Figure 1(a). Initially, steps dimensions are calculated by equating the perimeter 'P' of Antenna 3 with circumference 'C' of circular monopole. In Antenna 3 perimeter 'P' is calculated using (2), as $C = P$ where

$$\begin{aligned} C &= 2 \times \Pi \times R \\ P &= (\Pi \times R) + (2 \times R) + (4 \times \text{Step height}) \end{aligned} \tag{2}$$

Equating 'P' and 'C' results in steps height of 2.9 mm. Increase in path length results in the improvement of impedance bandwidth at lower frequencies, but mutual coupling degrades due to reduction in inter-element spacing.

A circular metallic reflector is further introduced in the ground plane to reduce the mutual coupling

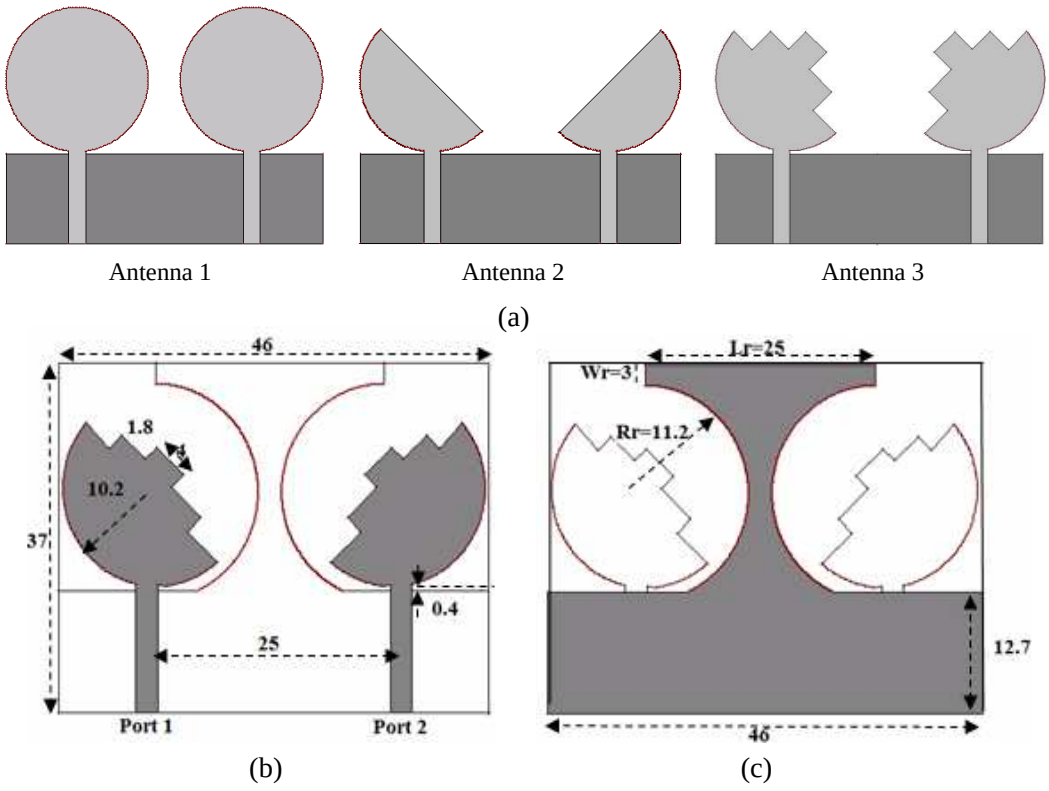

Figure 1. Antenna geometry, (a) evolution of proposed structure, (b) top view, and (c) bottom view of proposed structure (all dimensions are in mm).

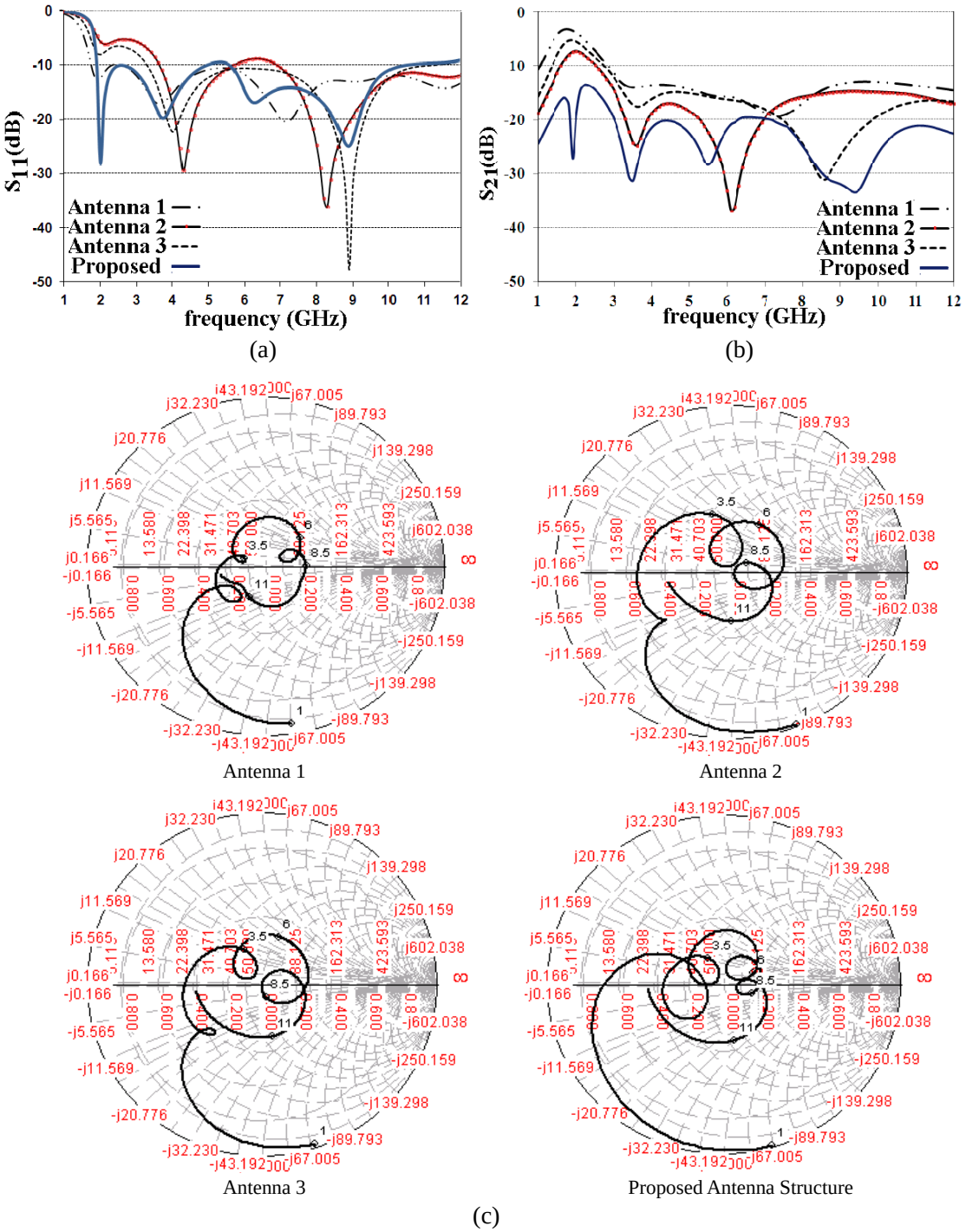

Figure 2. Simulated (a) S_{11} and (b) S_{21} of all structures, (c) impedance plots.

between the elements and to improve the impedance bandwidth. The circular shaped metallic reflector supports multiple modes with each mode having wide bandwidth and thus reduces mutual coupling over ultra-wide bandwidth [19]. It is basically an extension of the ground plane. The radius of extended ground plane R_r is calculated to be 13.7 mm using (1) for lower resonant frequency of 2 GHz. However, reflector of $R_r = 13.2$ mm cannot be accommodated with inter-element spacing of 25 mm. Therefore, the reflector is modified by introducing a rectangular strip of dimension $L_r \times W_r$. The optimized dimensions

of reflector are $R_r = 11.2$ mm, $W_r = 3$ mm and $L_r = 25$ mm. Beside this, steps dimensions are optimized to height and length of 1.8 mm and 4 mm respectively.

Now to improve return loss, the feed lines are offset by 0.5 mm, and gap 'g' is optimized to 0.4 mm to achieve impedance matching over the 2.0 GHz–10.6 GHz band in order to cover Bluetooth, Wi-Fi, Wi-MAX and UWB frequency bands. As a result, not only is S_{11} less than -10 dB over 2 GHz–10.6 GHz frequency band, but mutual coupling between the elements also decreases considerably. Mutual coupling less than -14 dB and less than -20 dB are achieved over the 2 GHz–3 GHz band and UWB, respectively. The optimized dimensions of the proposed antenna structure are mentioned in Figures 1(b) and (c).

Mutual coupling or isolation between the two elements can be studied using surface current distribution. Port 1 of the structure is fed while port 2 is terminated with a matched load. Current distributions at 2 GHz, 4 GHz, 7 GHz and 10 GHz are shown in Figure 3. Surface current distribution

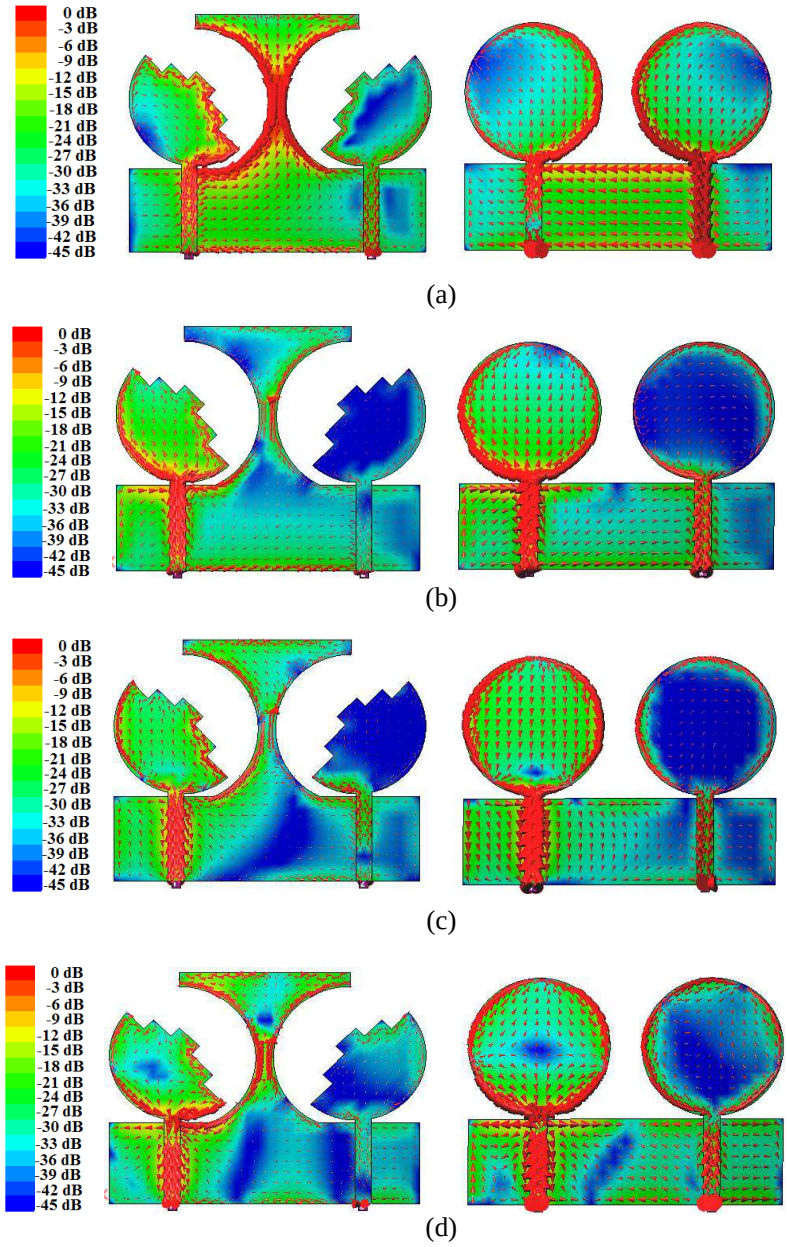

Figure 3. Surface current distribution of proposed structure and antenna 1 at (a) 2 GHz, (b) 4 GHz, (c) 7 GHz, (d) 10 GHz.

shows that the current induced in the second element of the proposed antenna structure is considerably reduced compared to Antenna 1.

3. FABRICATIONS AND MEASUREMENTS

3.1. Impedance Performance and Isolation Mechanism

A photograph of the fabricated MIMO diversity antenna is shown in Figure 4. S_{11} and S_{21} of the proposed antenna structure are measured using Vector Network Analyzer ET 8722. Figures 5(a) and 5(b) show the simulated and measured S_{11} and S_{21} of the antenna structure, respectively. The measured results are in agreement with the simulated ones. It is observed that measured S_{21} is less than -20 dB and -14 dB for UWB and 2 GHz–3.1 GHz, respectively.

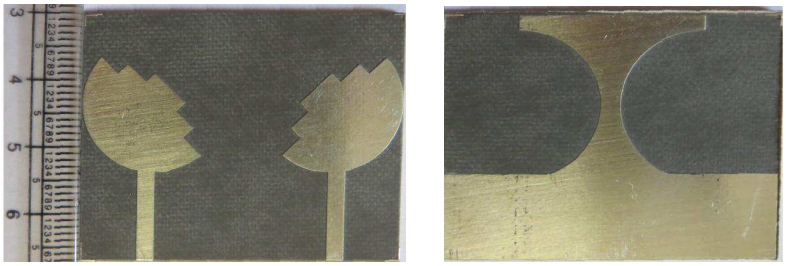

Figure 4. Fabricated prototype of the proposed antenna structure.

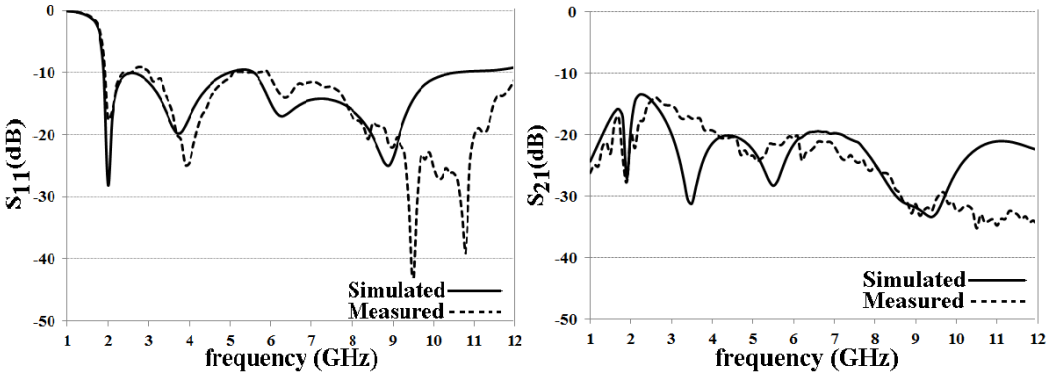

Figure 5. Measured and simulated (a) S_{11} and (b) S_{21} of proposed structure.

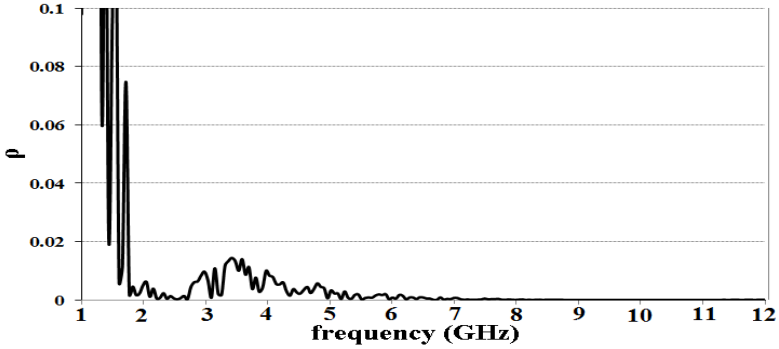

Figure 6. Correlation coefficient calculated using measured scattering parameters.

3.2. Diversity Performance

Pattern diversity is used to reduce the channel fading caused by multipath environments. The envelope correlation coefficient is a important parameter to judge the diversity performance of antenna. Correlation coefficient is calculated using S parameters. For a two-port antenna system, using uniform

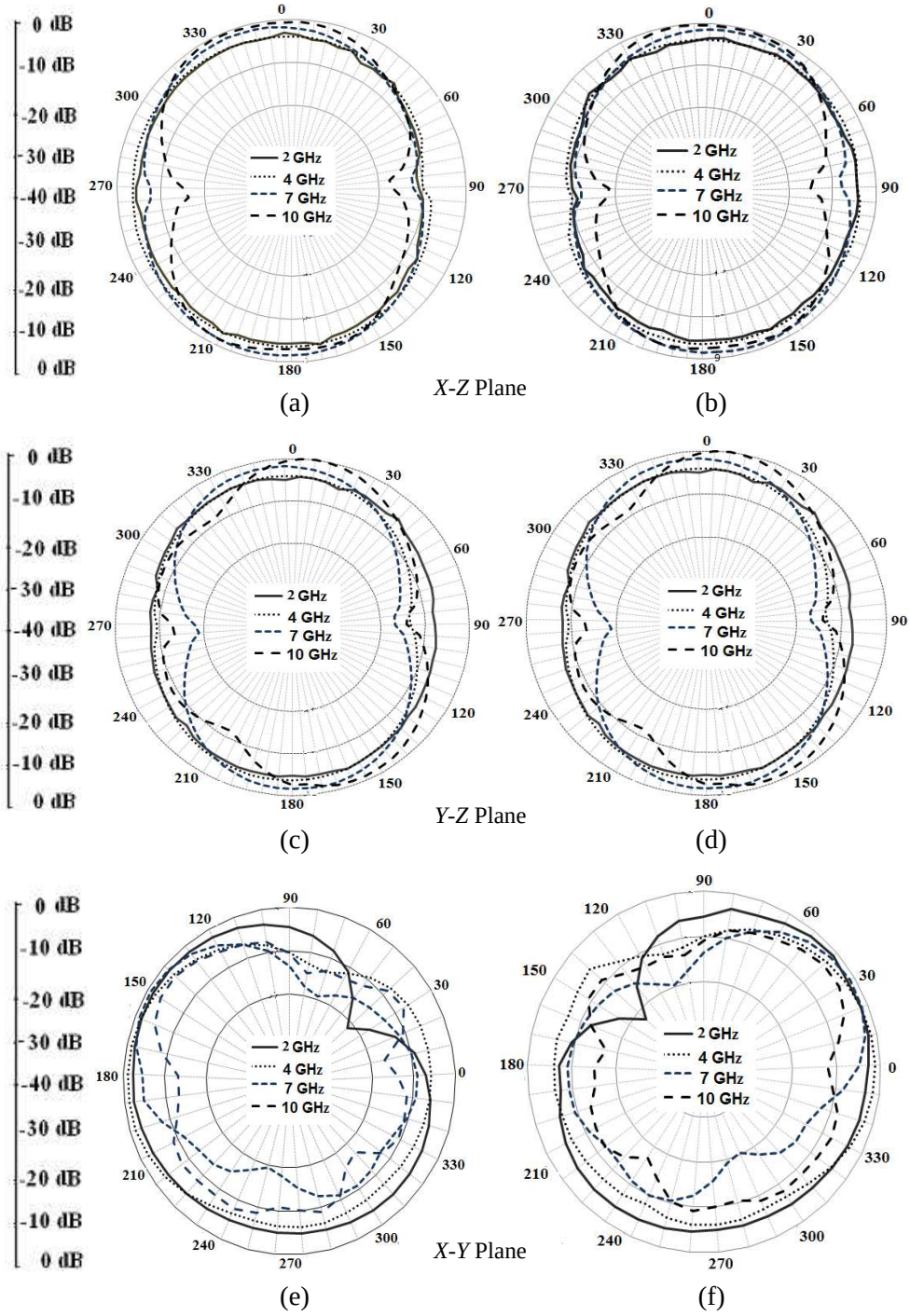

Figure 7. Measured radiation patterns of antenna at port 1, (a) X-Z plane, (c) Y-Z plane, (e) X-Y plane and antenna at port 2, (b) X-Z plane, (d) Y-Z plane, (f) X-Y plane of proposed structure.

multipath environment the correlation is calculated using (3) [22]

$$\rho = \frac{\left| \iint_{4\pi} \left[\vec{F}_1 (\Theta, \Phi) \cdot \vec{F}_2 (\Theta, \Phi) \, d\Omega \right] \right|^2}{\left| \iint_{4\pi} \left[\vec{F}_1 (\Theta, \Phi) \, d\Omega \right] \right|^2 \left| \iint_{4\pi} \left[\vec{F}_2 (\Theta, \Phi) \, d\Omega \right] \right|} \tag{3}$$

where F_1 (θ, Φ) is the field radiation pattern of the antenna when port 1 is excited, and ($\cdot$) is the hermitian product. Equation (4) is a simplified form of (3) [22]. It uses equivalent S parameters to calculate the correlation coefficient

$$\rho = \frac{\left| S_{11}^* S_{12} + S_{21}^* S_{22} \right|^2}{\left(1 - \left(|S_{11}|^2 + |S_{21}|^2 \right) \right) \left(1 - \left(|S_{22}|^2 + |S_{12}|^2 \right) \right)} \tag{4}$$

It is considered that significant diversity is achieved if the correlation coefficient is less than 0.5 [23]. Figure 6 shows the correlation coefficient calculated using measured S parameters of the proposed structure. Correlation coefficient less than 0.02 is achieved throughout the band which is significantly less than the correlation coefficient required for good diversity performance. The diversity gain is calculated using (5)

$$G_{app} = 10 \times \sqrt{1 - |\rho|} \tag{5}$$

The calculated diversity gain is more than 9.99 dB throughout the frequency band 2 GHz–10.6 GHz.

3.3. Radiation Characteristics

The measured radiation patterns at 2 GHz, 4 GHz, 7 GHz and 10 GHz in three principal planes $\Phi = 0°$, $\Phi = 90°$ and $\theta = 90°$ which correspond to x-z plane, y-z plane and x-y plane, respectively, are shown in

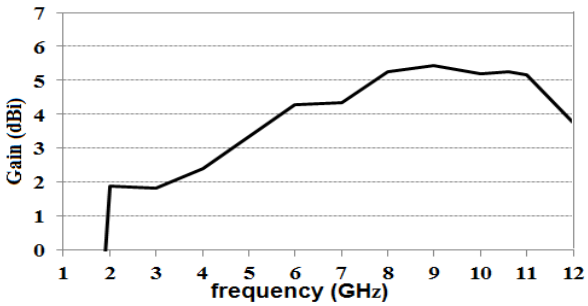

Figure 8. Measured gain of antenna at port 1 with port 2 match terminated.

Table 1. Comparison of the proposed antenna with references.

Ref.	Size (mm^2)	S_{21} (dB)/Isolation	$f_L - f_H$ (GHz)
[8]	68×40	-15	3.1–10.6
[9]	62×38	23	3.1–10
[10]	91×38	-17	3.1–10.6
[11]	35×40	-16	3.1–10.6
[12]	35×40	20	4.4–10.7
[13]	25×40	26	3.1– 5.15
[14]	37×45	20	3.1– 5.0
PS	46×37	-14 (2.0–3.1 GHz)	2.0–10.6
		-20 (3.1–10.6 GHz)	

PS — Proposed Structure.

Figure 7. For measurements, port 1 is excited while port 2 is terminated with 50 Ω load. The radiation patterns are relatively stable over impedance bandwidth. The radiation patterns in x-z and x-y planes for both antennas are mirror image of each other with respect to y-z plane. The measured antenna gain is shown in Figure 8. Gain variation less than 3.5 dB is observed over 2.0–10.6 GHz.

Table 1 gives the detailed comparison of the proposed structure with other references. It can be seen that the results of the proposed structure are good in terms of bandwidth, isolation and size.

4. CONCLUSION

A MIMO diversity antenna for Bluetooth, Wi-Fi, Wi-MAX and UWB applications is proposed. A circular shape reflector at ground with 90° angularly separated semicircular monopole with steps is presented. The antenna structure is designed, fabricated and tested. Measured results show reasonable agreement with simulated ones. S_{11} less than −10 dB is achieved over 2 GHz–10.6 GHz. S_{21} less than −20 dB and −14 dB are achieved for UWB and 2 GHz–3.1 GHz, respectively. Correlation coefficient less than 0.02 is achieved throughout the band. The proposed antenna features stable radiation patterns throughout the band.

REFERENCES

1. Andersen, J. and H. Rasmussen, "Decoupling and descattering networks for antennas," *IEEE Trans. Antennas Propagation*, Vol. 24, No. 6, 841–846, Nov. 1976.
2. Yang, F. and Y. Rahmat-Samii, "Microstrip antennas integrated with electromagnetic band-gap (EBG) structures: A low mutual coupling design for array applications," *IEEE Trans. Antennas Propagation*, Vol. 51, No. 10, 2936–2946, Oct. 2003.
3. Ramon, G., P. Maagt, and M. Sorolla, "Enhanced patch-antenna performance by suppression surface waves using photonic-bandgap substrates," *IEEE Trans. Microw. Theory Tech.*, Vol. 47, No. 11, 2131–2138, 1999.
4. Salehi, M., A. Motevasselian, A. Tavakoli, and T. Heidari, "Mutual coupling reduction of microstrip antennas using defected ground structure," *10th IEEE Singapore International Conference on Communication systems*, 1–5, 2005.
5. Xiao, S., M.-C. Tang, Y.-Y. Bai, S. Gao, and B.-Z. Wang, "Mutual coupling suppression in microstrip array using defected ground structure," *IET Microwaves, Antennas & Propagation*, Vol. 5, No. 12, 1488–1494, May 2011.
6. Bait-Suwailam, M. M., M. S. Boybay, and O. M. Ramahi, "Electromagnetic coupling reduction in high-profile monopole antennas using single-negative magnetic metamaterials for MIMO applications," *IEEE Trans. Antennas Propagation*, Vol. 58, No. 9, 2894–2902, Sep. 2010.
7. Khaleela, H. R., H. M. Al-Rizzob, D. G. Rucker, Y. A. Rahmatallahb, and S. Mohan, "Mutual coupling reduction of dual-band printed monopoles using MNG metamaterial," *IEEE International Symposium on Antennas and Propagation (APSURSI)*, 2219–2222, 2011.
8. Najam, A., Y. Duroc, and S. Tedjni, "UWB-MIMO antenna with novel stub structure," *Progress In Electromagnetics Research C*, Vol. 19, 245–257, 2011.
9. Li, Y., W. X. Li, C. Liu, and T. Jiang, "Two UWB-MIMO antennas with high isolation using sleeve coupled stepped impedance resonators," *2012 IEEE Asia-Pacific Conference on Antennas and Propagation*, 21–22, Singapore, Aug. 27–29, 2012.
10. Jusoh, M., M. F. Jamlos, M. R. Kamarudin, and F. Malek, "A MIMO antenna design challenges for UWB application," *Progress In Electromagnetics Research B*, Vol. 36, 357–371, 2012.
11. Zhang, S., Z. Ying, J. Xiong, and S. He, "Ultrawideband MIMO/diversity antennas with a tree-like structure to enhance wideband isolation," *IEEE Antennas And Wireless Propagation Letters*, Vol. 8, 1279–1282, 2009.
12. Prasanna, K. M. and S. K. Behera, "Compact two-port UWB MIMO antenna system with high isolation using a fork-shaped structure," *2013 International Conference on Communications and Signal Processing (ICCSP)*, Vol. 8, 726–729, 2009.

13. Zhang, S., B. K. Lau, A. Sunesson, and S. He, "Closely-packed UWB MIMO/diversity antenna with different patterns and polarizations for USB dongle applications," *IEEE Trans. Antennas Propagation*, Vol. 60, No. 9, 4372–4380, Sep. 2012.
14. See, T. S. P. and Z. N. Chen, "An ultrawideband diversity antenna," *IEEE Trans. Antennas Propagation*, Vol. 57, No. 6, 1597–1605, Jun. 2009.
15. Reddy, G. S., A. Chittora, S. Kharche, and J. Mukherjee, "Bluetooth/UWB planar diversity antenna with WiMAX and WLAN band-notch characteristics," *Progress In Electromagnetics Research B*, Vol. 54, 303–320, 2013.
16. Najam, A. I., Y. Duroc, S. Tedjini, and J. F. A. Leao, "A novel co-located antennas system for UWB MIMO applications," *IEEE Radio and Wireless Symposium, RWS' 09*, 368–371, Jan. 18–22, 2009.
17. Najam, A. I., Y. Duroc, and S. Tedjini, "Design and analysis of MIMO antennas for UWB communications," *Proceedings of the Fourth European Conference on Antennas and Propagation (EuCAP)*, 1–5, Apr. 12–16, 2010.
18. IE3D Release 14, Zeland Software Inc., Fremont, CA, USA, 2008.
19. Kumar, G. and K. P. Ray, *Brooadband Microstrip Antennas,* Artech House, Norwood, MA, 2003.
20. Mishra, S. K., R. K. Gupta, A. Vaidya, and J. Mukherjee, "1×3 microstrip line-fed metal-plated split U shaped omnidirectional ultra-wideband monopole antenna," *IETE Journal of Research*, Vol. 58, No. 5, 429–434, Sep.–Oct. 2012.
21. Ahmed, O. M. H. and A.-R. Sebak, "A printed monopole antenna with two steps and a circular slot for UWB applications," *IEEE Antennas and Wireless Propagation Letters*, Vol. 7, 411–413, 2008.
22. Blanch, S., J. Romeu, and I. Corbella, "Exact representation of antenna system diversity performance from input parameter description," *Electron. Lett.*, Vol. 39, No. 9, 705–707, May 2003.
23. Ko, S. C. K. and R. D. Murch, "Compact integrated diversity antenna for wireless communications," *IEEE Trans. Antennas Propagation*, Vol. 49, No. 6, 954–960, 2001.